Enhancing Ignition by Conditioning the Fast-Spark Induced Flow Field

A.Borghese, M.Diana*, V.Moccia and R.Tamai

Istituto Motori, CNR
Via Marconi, 8
80126 Napoli
Italy
* *Università Federico II*

ABSTRACT

The physical processes induced by a very fast spark discharge in quiescent propane/air mixtures have been observed by 2-D laser shadowgraphy and 1-D Rayleigh Laser light Scattering techniques. The temporal evolution and spatial distribution of the heated gases, previously described by a model, are presented and linked to the shape transition of the shock wave fronts. The build-up and the evolution of an associated flow field has been followed, evidencing the morphological transition of the excited gas pocket, leading to toroidal flame fronts.

The different behaviours of inert and reactive mixtures have allowed us to attribute the radial enlargement of the excitation to the fast spark and the isotropic expansion to the chemistry. Preliminary investigations were carried out in order to exploit the turbulent flow field induced by the fast spark.

INTRODUCTION

Spark-ignition of hydrocarbon/air mixtures is a topics of relevant interest in the technology of s.i. engines, operated in the so-called 'lean burn' mode. The reasons for that are assumed to be well known and will not be discussed here.

In order to reach more reliable and effective ignition in these conditions, it has been realized that deeper fundamental knowledge of the physical processes involved is required, which can lead to the development of devices, based on new concepts and effects.

Now, the ignition of inflammable gas mixtures by means of electric sparks is a complex phenomenon, involving concurrent and interacting mechanisms, such as plasma excitation and relaxation, fluid dynamic perturbations and combustion chemistry. This is particularly true in the case of very short and intense sparks, which have shown attractive features as sources for 'enhanced' ignition (1-5).

From a more fundamental point-of-view, their short duration helps to keep the excitation phase and the subsequent evolution of the excited gas apart, whereas the delivered energy is channeled not only to the excited states of the chemical species, but also to the build-up of a locally intense flow field.

The aims of this work are to report experimental descriptions of thermal and fluid dynamic excitations and to highlight their effects and interactions.

EXPERIMENTAL SET-UP AND TECHNIQUES

The experiments are carried out in a constant-volume combustion bomb, operated with propane/air mixtures with different equivalent ratios ϕ. The propane/air mixtures are prepared by injection of well controlled amounts of sprayed liquid fuel into the transient air flow, during the filling up of the chamber from vacuum to 200 kPa.

A fast H.V. pulser, based on that described in (2), provides short and intense sparks between two 1mm-spaced electrodes.

The combustion chamber is provided with optical accesses through quartz windows in order to allow time- and space-resolved laser diagnostics, as specified below.

Shadowgraphy and one-dimensional 'imaged' Rayleigh Light Scattering (RLS) have been applied, in order to have 2-D qualitative and 1-D quantitative visualization, respectively, of the phenomena, over four time decades (0.2-2000 μs) of spark-to-laser pulse delays.

An optical shutter, described in (6), replaces the quartz window in the RLS experiments.

The availability of the imaged RLS technique allowed us, in addition, to control the degree of homogeneity of mixing of propane and air.

Extensive details of the experimental apparatus and of the diagnostic scheme are given in (4) and (6).

THE SOURCE OF THE EXCITATION

Throughout the present work, by the term 'excitation' we mean the complex physical state of the gaseous system, occurring after a fast release of electric energy (spark discharge) and which either relaxes in time and space, as in inert gases, or develops toward self-sustained combustion, as in reacting mixtures.

In our experiments, the source of the 'excitation' is an electric spark discharge, very fast (~100ns duration) and yet very intense (~1MW peak power,~20-40mJ energy). From previous spectroscopic measurements (2, 3), it has been shown that a plasma channel develops within the first tens of nanoseconds, with very high electron temperatures and densities and then relaxes to neutral conditions within the first microsecond.

The fast energy release gives rise also to a strong shock wave, which initially envelops the roughly cylindrical hot gas kernel, then detaches and propagates outward, approaching asymptotically a spherical shape.

It has been shown (7,8) that the propagation law of the shock front along the equatorial plane of symmetry can be accurately described by a simple analytical relationship:

$$R_{sh}^2=R_o^2+kt+c^2t^2 \qquad (1)$$

where R_{sh} and t are the distance of the shock front from the spark axis and the time, respectively; the three parameters of the fit are interpreted as follows: Ro is an equivalent 'zero-time' dimension of the kernel, taking into account the finite spark duration and its energy; k is a quantity, allowing for the transient behaviour of the shock; finally, c is the third parameter which reproduces fairly well in the fit the value of the sound speed; as a result, the initial, transient and asymptotic propagation terms combine according to the sum of the squares of corresponding 'distances'. The empirical meaning of the 'k' parameter in Eq.1 reflects the findings of the 'blast wave' theory in the self-similar formulation (9), which predicts, in cylindrical symmetry, a linear dependence of R_{sh}^2 upon the time and the square root of the istantaneously released spark energy.

Based upon the above described analytical fit of experimental data, a model, described in (8), has been developed by solving the appropriate conservation equations, with boundary conditions derived by Eq.1 and the associate Rankine-Hugoniot relationships. Figures 1.A,B,C show the main results, namely the computed radial profiles of the main physical quantities (A), species concentrations (B) and energy distributions (C) at 100 ns from the spark onset. It is worth noting that, despite the extremely high temperatures of the inner core of the plasma channel, the most part of the energy is entrapped by neutral

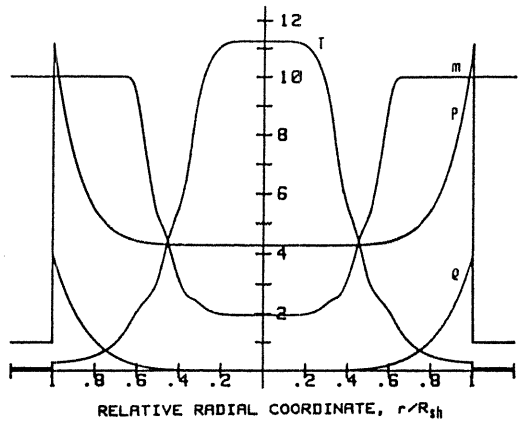

Fig.1.A - Computed radial distribution of gas density (1.16 Kg m^{-3}/div), pressure P (1 bar/div), temperature T (3000 K/div) and mean molecular weight m (2.9 g $mole^{-1}$ /div) for t=100 ns after spark onset; pure nitrogen at 1 bar and room temperature (from Ref. 8).

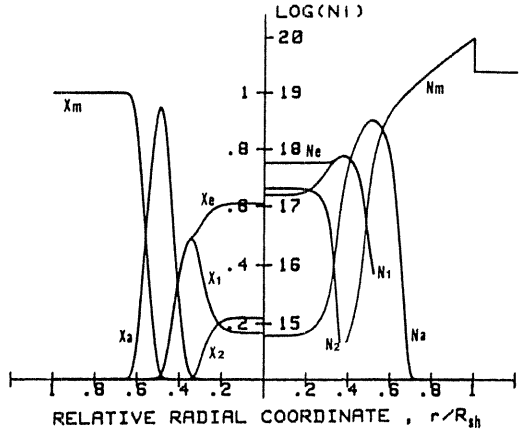

Fig. 1.B - Computed radial distribution of molar fractions X_i (left) and number concentrations N_i (right) of molecules (m), atoms (a), first N-ions (1), second N-ions (2), electrons (e) respectively. Same conditions as in Fig.1A (from Ref.8).

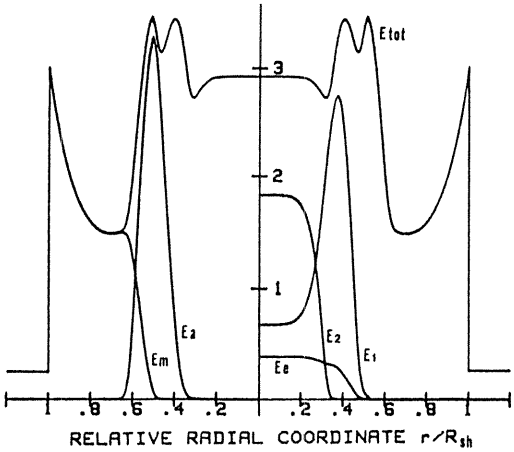

Fig. 1.C - Computed radial distributions of internal energy density terms E_i (10^6 Jm^{-3}/div). Conditions and notations as in Fig. 1B (from Ref. 8).

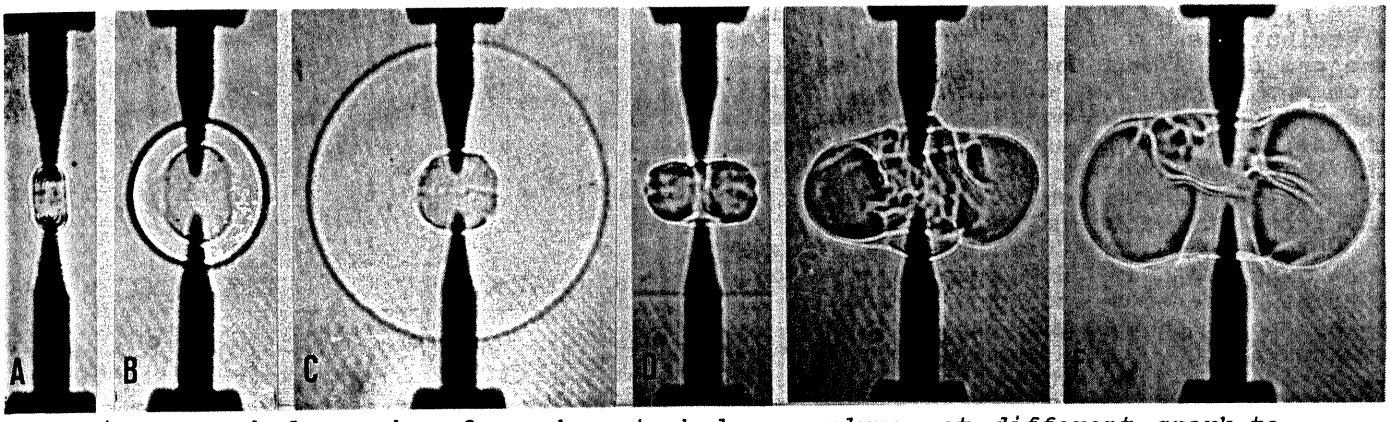

Fig. 2 - Shadowgraphs of spark-perturbed gas volume, at different spark-to-laser delays; A: 0.35 μs, B: 2.66 μs, C: 8.43 μs, D: 26.6 μs, E: 266 μs, F: 474 μs. P=200 kPa (2 bar), stoichiometric C_3H_8/air mixture (ø=1.0), E~20 mJ, electrode gap = 1mm.

species, at much lower temperatures, which constitute the outer shell of the channel. The model predicts also an overall energy content that reproduces closely the experimental value.

THE DEVELOPMENT OF THE EXCITATION

Following the plasma phase, the spatial distributions of the physical quantities, as predicted by the above mentioned model, undergo temporal evolutions, in terms of both a thermal relaxation of the hot gases and the simultaneous development of a gas flow field.

The main support to the investigations in this time phase comes from the combination of experimental data of qualitative, 2-D visualization by laser shadowgraphy, and quantitative, 1-D 'imaging' by laser light scattering technique, both providing excellent time- and space-resolution.

Figures 2.A-F show a selection of laser shadowgraphs, at increasing spark-to-laser delays, as specified in the caption. The density gradients evidenced document the evolution of the spatial perturbations induced by the spark.

Firstly, in the time phase 0.2-20 μs, the shock wavefront propagates outward and also undergoes a shape transition, namely from a roughly cylindrical shape, at very early times, to an ellipsoidal one with decreasing eccentricity, later on (Fig.2.A-C).

Furthermore, the hot gas pocket, confined closely by the shock front at its onset and detached at about 1 μs, shows a topological transition from a rod-like contour to a toroidal, doubly connected domain within the following 100 μs.

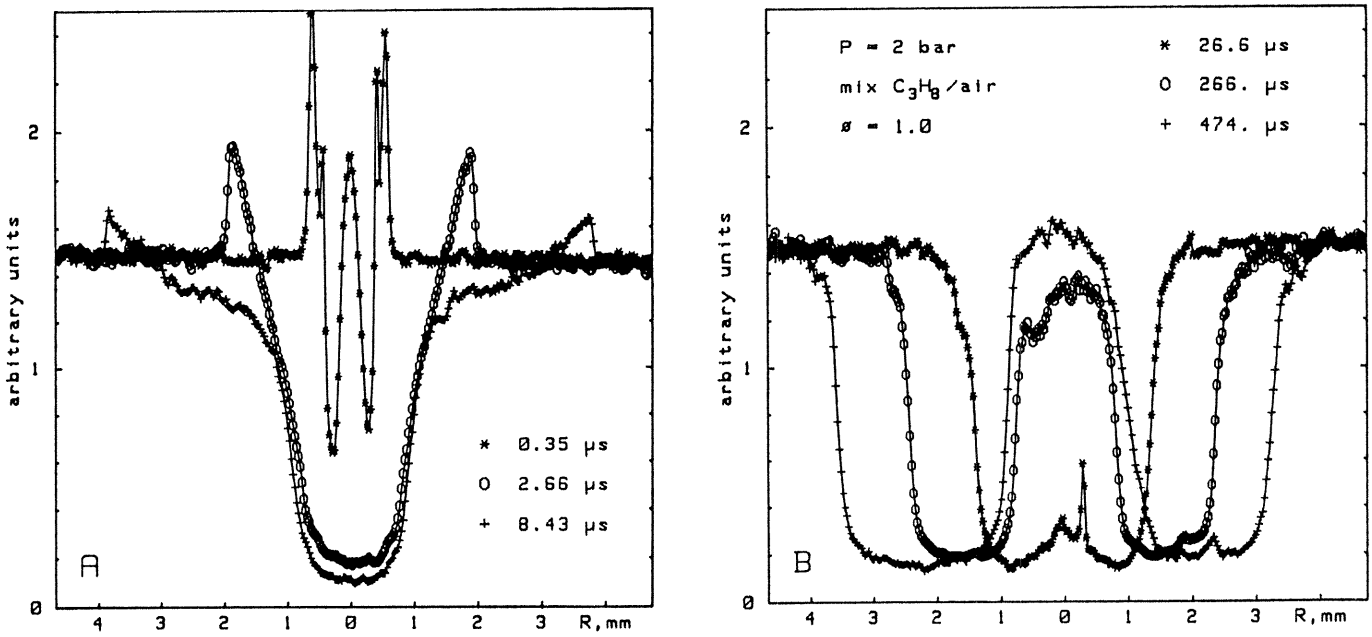

Fig. 3 - Single-shot, Rayleigh laser Light Scattering radial patterns, normalized to the unperturbed air signal (4). Same conditions as in Fig. 2.
A: (*) 0.35 μs, (o) 2.66 μs, (+) 8.43 μs
B: (*) 26.6 μs, (o) 266 μs, (+) 474 μs.

Figures 3.A,B show the radial distributions on the equatorial plane of the gas density at the corresponding times from the spark, as obtained by 'imaged' laser light scattering (6). The deep wells in the radial patterns in Fig.3.A evidence the hot gas kernel, whereas the sharp, symmetrical peaks denote the position and the intensity of the shock front.

In Fig.3.B the density profiles show the expansion of the outer hot front, whereas a density recovery occurs in the axial zone, supporting the evidence of recirculating cold gases entering the electrode gap from outside.

The build-up of observed gas flow field can be related to the peculiar dynamics of the shock, as described below.

Accurate inspection of shadowgraphs in the time window 0.2-20 μs has revealed that the shock front changes progressively its shape, so that it describes approximately a family of confocal ellipsoids, whose eccentricity decreases at increasing times. The conjugate family of hyperboloids, with the same foci, represent in this frame, the locus of all the trajectories, along which the collisions among gas molecules propagate the shock. Now, these trajectories are hyperbolas, with higher curvatures occurring closer to the foci and, hence, at earlier times. Thus, the gas molecules, sequentially involved, collide and move so that a flow field is traced, acting so to give rise to a couple of symmetrical cyclonic circulations, each surrounding the tip of one electrode and oriented so to push inward-propagating axial gas flows and to eject gases outward on the equatorial plane.

THE TRANSITION TO COMBUSTION

The shadowgraphs and light scattering data do not reveal significant differences in the observed behaviour of inert vs. reacting mixtures, within the first 100 μs, although in the latter case some sort of chemical activity is likely to occur. The bifurcation of behaviours is, instead, observed after this time, as shown in the series of shadowgraphs of Fig.4.A,B where inert (A) and reactive conditions (B) are reported.

Whereas excitation of inert gases results in a chaotic relaxation of the flow field within some hundreds of microseconds, combustion fronts are clearly evidenced in reacting mixtures, exhibiting noticeable and peculiar toroidal contours. The corresponding LLS data, shown in Fig.3.B, provide quantitative informations about speed, thickness and temperature of the growing flame, on the equatorial plane. Here it is worth noting that, while the outer flame front travels at this stage with a speed of about 4 m/s, the inner edge has moved a quite small distance, despite the fact that the advantageous flame geometry (locally concave surface) should result in flame speeds higher than in the 'convex'

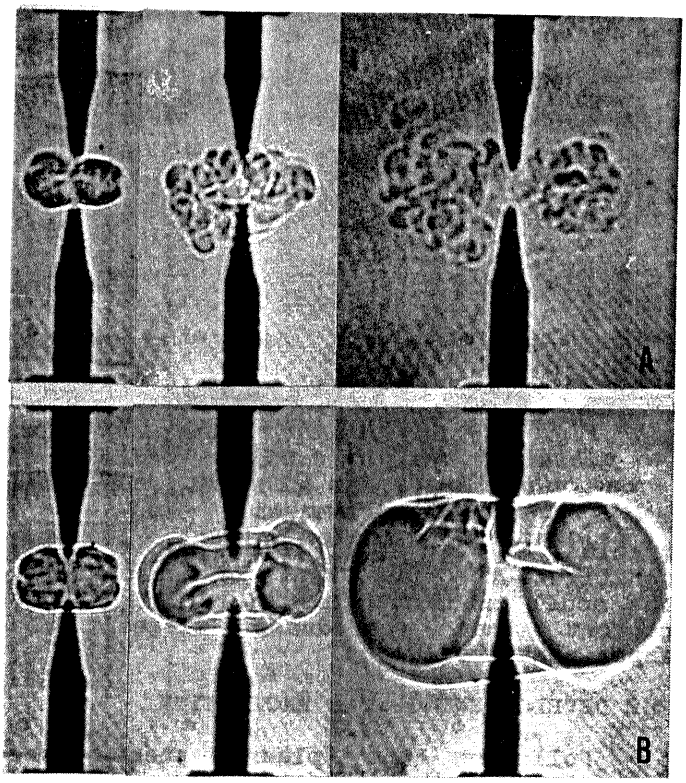

Fig. 4 - Shadowgraphs in air (A: ø=0.0) and in stoichiometric C_3H_8/air mixture (B: ø=1.0) at three spark-to-laser delays; left: 20 μs, center: 150 μs, right: 632 μs.

case; reasonably, it can be derived that the 'recirculation' flow field feeds with fresh gases the inward-propagating flame front, resulting in its apparent 'surplace'.

The persistence of the shapes up to about 2000 μs allows to carry out a geometrical analysis of the flame growth. As far as the flame front can be described by a regular toroidal surface, with major radius a and a cross-section with radius b, it is possible to plot them as functions of the time and of the equivalence ratio ø as reported in Fig.5.A,B .

The behaviour of the radius a(t), which reflects the radial expansion, after a fast jump at earlier times, keeps constant and unaffected by the chemical reactivity, thereby suggesting to be 'driven' mainly by the spark-induced fluid dynamics; on the other hand, b(t) (the isotropic expansion of the flame) shows a monothonic increase as well as a dependence on the equivalence ratio, revealing to be 'driven' by the chemistry.

VARYING INITIAL AND BOUNDARY CONDITIONS

The findings outlined above reflect mostly the dependence of the morphology and the dynamics of the excited gas pocket upon a given kind of spark discharge, in an un-confined environment. Now, questions can be addressed about whether and how much the kind of spark and the boundary conditions affect the phenomena observed.

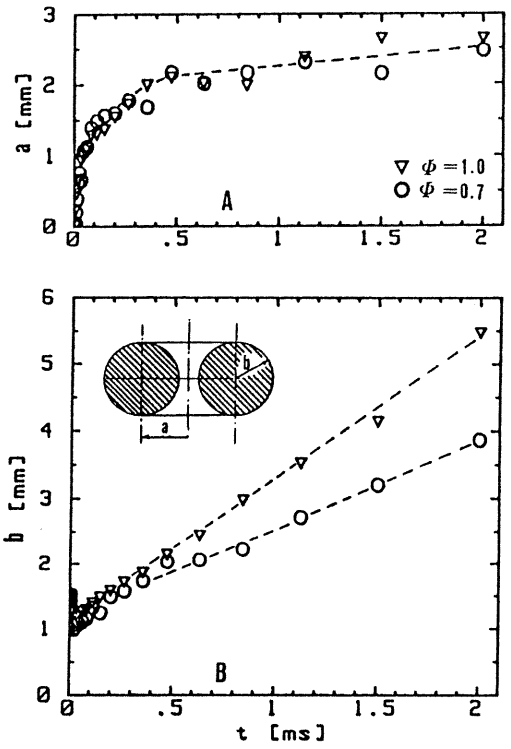

Fig. 5 - Radii of the equivalent tore, a (A), and of its circular cross-section, b (B), as functions of time, inferred by shadowgraphs at ø=1.0 (▽) and ø=0.7 (○). Same operating conditions as in Fig. 2.

Accordingly, a fast capacitive spark (~100 ns duration,~30 mJ energy) and a glow discharge from an ignition coil (1-2 mJ,20 ns plus ~ 30 mJ,3 ms) have been used alternatively to excite the gas; the resulting shock wave propagation is reported in Fig.6 for the two cases; larger initial kernel and higher shock speed of the fast spark are observed, as quantitatively predicted by the Eq.1 when much higher energy is delivered in the break-down phase (7, 8).

The visualization of the corresponding flow fields is given in Fig.7.A,B ; the presence and the positions of the two vortices, predicted above, are clearly evidenced in the case of the weaker spark (A), whereas these features are even obscured in (B), due to the much stronger excitation.

Further indications have been derived by considering different boundary conditions for the spark excitation; so far, only two idealized, limiting cases have been explored: in the first one, the gas excitation is allowed to expand only in a half-space, obtained by inserting a PTFE plate in close contact to the electrodes; the resulting effects have been qualitatively analyzed and compared to the un-confined geometry. Figure 8 shows the gas excitation at t=356 μs for the two cases, and documents the additional perturbation on both flame front and structure, deriving by the 'mirror' effect of the plate.

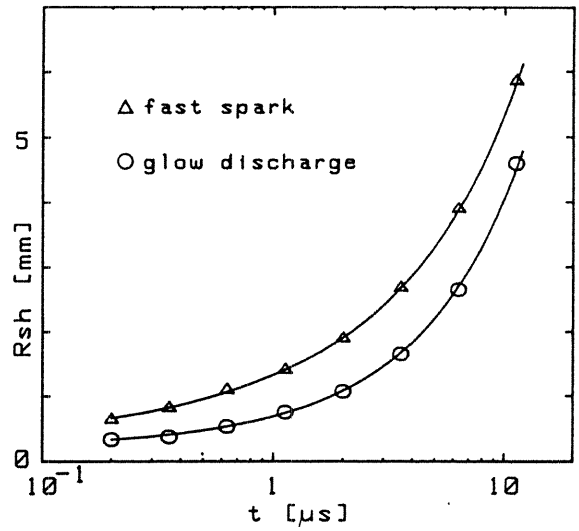

Fig. 6 - Radial position of the shock fronts as function of time. Experimental: (Δ) fast spark 30 mJ, 100ns; (○) composite spark (1-2 mJ, 30 ns followed by a glow discharge 30mJ, 3ms). The best fits of the two sets of data with Eq. 1 are plotted by continuous line; the values of the coefficients are respectively:
f. spark: R_o=.35mm k=1.5mm^2/μs c=.365mm/μs
glow dis: R_o=.20mm k=0.3mm^2/μs c=.365mm/μs

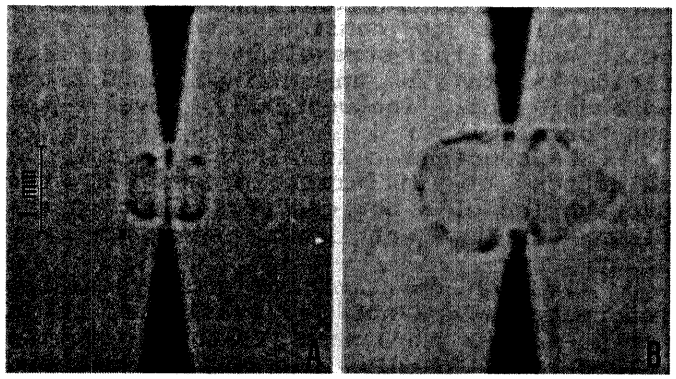

Fig. 7 - Shadowgraphs at t=11.2 μs for the composite spark (A) and the fast spark (B), as defined in Fig. 6.

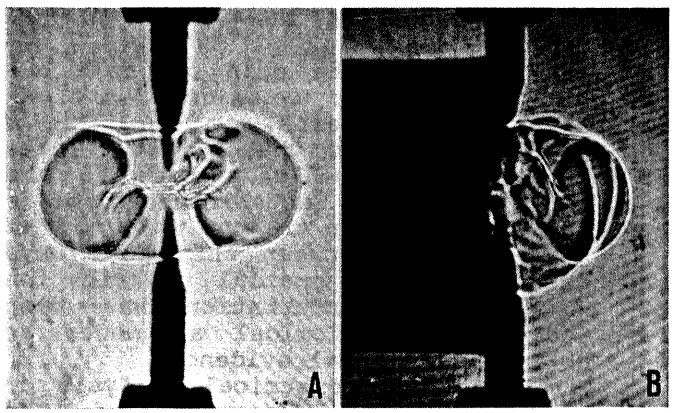

Fig. 8 - Shadowgraph at t=356 μs corresponding to an unconfined (A) and a partially confined (half-space) spark (B). Same conditions as in Fig. 2.

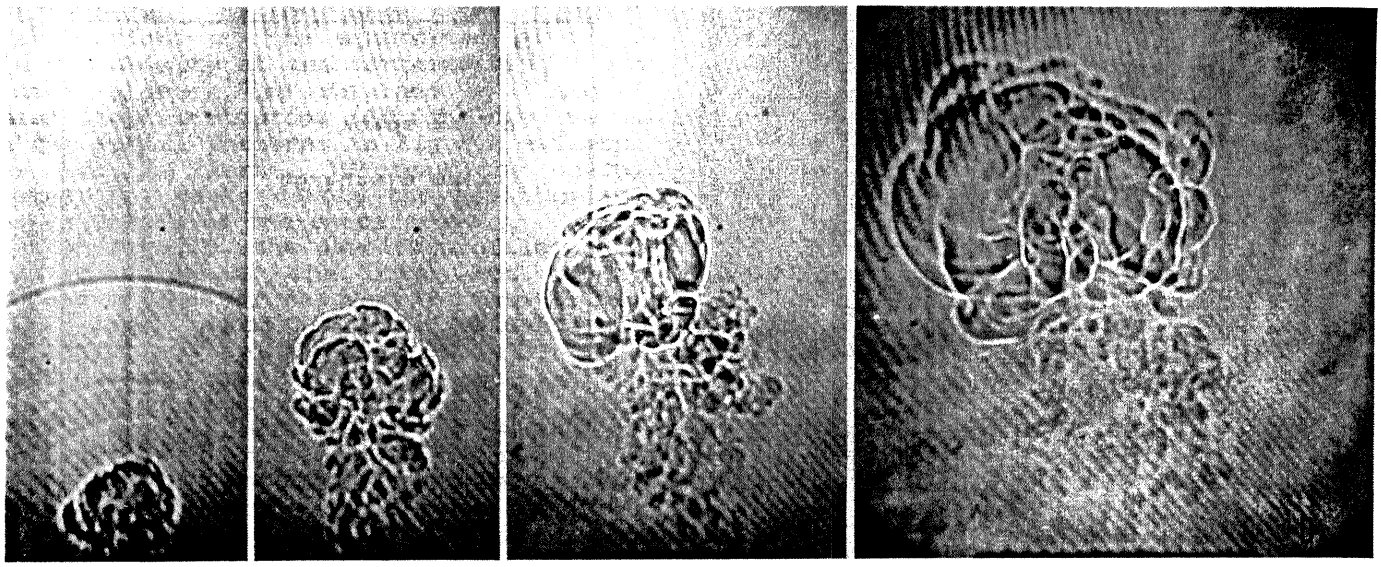

Fig. 9 - Shadowgraphs of gas volumes, excited by fully confined sparks ('plasma-jets') at four diferent time delays; A: 20 μs, B: 84 μs, C: 266 μs, D: 632 μs. Plasma-jet cavity ~2 mm^3, orifice diameter = 1 mm, E ~25 mJ. Other conditions as in Fig. 2.

A quite different, yet more meaningful situation refers to the fast-spark excitation of a small gas pocket, enclosed in a cylindrical cavity (~2 mm^3 volume), in much the same way as in 'plasma-jet' geometries of Ref.10. Here, the idea is to confine within a small solid angle the streamlines of the flow field, which in un-confined conditions spreads out isotropically over the equatorial plane.

Shadowgraphs in Fig.9 show a selection of different stages of the propagation of a hot gas pocket out of the plasma cavity at four spark-to-laser delays.

Although quantitative and systematic informations are not yet available, it is worth noting the main features of the pulsed jet, namely its high speed and persisting turbulence level, which incidentally turned out to be even excessive for successful ignition in lean mixtures.

DISCUSSION AND CONCLUSIONS

In this work the main emphasis has been put on the fluid dynamics of the gas excitation by fast sparks.

It has been shown that a fast release of electrical energy leads both to the heating and to the establishment of a peculiar flow-field in the gas medium.

A connection between the shock wave propagation and the spatial distribution of the induced perturbation has been revealed, by morphological arguments as well as by experimental evidence.

A simplified geometrical analysis of the flame fronts has suggested the attribution of distinct causes, i.e. the fast spark and the combustion chemistry, to the growth factors a(t) and b(t) of the toroidal flames observed. In this interpretation scheme, some questions can be raised about whether and to what extent the combustion-driven expansion can sustain or even enhance the 'recirculation' flow field in the spark gap zone.

In connection with the observations of the ignition phenomena, it has been found that whether a spark excitation leads to propagation or extinction is decided well after the establishment of the toroidal flames; we propose here, as a hint for further investigations, to consider 'inflammability' criteria based upon topological arguments, namely to analyze the stability of flame fronts, to be meant as fronteers of many-fold connected domains.

In a wide sense, there is no doubt that the ignition spark cannot be thought of as a purely thermal excitation source, but as a trigger of complex phenomena, involving heating, recirculation and turbulent mixing of fresh and excited species, as well as combustion chemistry.

Preliminary attempts to modify the initial and the boundary conditions of the involved transient processes led to the following considerations.

The energy delivered to the gas in the break-down phase is responsible of the build-up of an initial 'ignition' nucleus and of an associated peculiar flow field, whose intensity and extent is a function of the energy amount.

Strictly speaking, the long-lasting tail of 'glow' discharges does not 'ignites', but rather feeds and sustains the initial flame kernel, ignited instead by the preceding spark.

From the preliminary experiments in confined geometries, we have been convinced that fluid dynamic modeling is essential to predict the involved effects; neverthless, we have shown that accurate qualitative visualization can help to derive useful indications as well.

However, the first indications suggest that proper confinement can lead to useful exploitation of spark-induced momentum, in order to produce turbulent mixing and desired displacement of the gas excitation.

In this frame, the combination of the 'fast sparks' and 'plasma jets' phenomenologies is in the perspective of considering plasma-jet igniters, requiring much less energy than in ordinary cases, due to the much faster depletion of the cavity and to the resulting much smaller losses to the cavity walls.

NOMENCLATURE

a = major radius of the tore, mm
b = radius of the tore cross section, mm
c = speed of sound, mm/μs
E = energy, mJ
E_i = energy density, J m^{-3}
m = mean molecular weight, g $mole^{-1}$
N_i = number concentration
P = pressure, kPa
R = radial coordinate, mm
t = time, s
T = temperature, K
X_i = molar fraction
ϱ = density, kg m^{-3}
ϕ = equivalence ratio

Subscripts

a = atomic
e = electronic
m = molecular
sh = shock
o = 'zero-time'
1 = first ionization
2 = second ionization

REFERENCES

1. Maly, R. and Vogel, M., "Ignition and Propagation of Flame Fronts in Lean CH_4-Air Mixtures by the Three Modes of the Ignition Spark", XVII Intern. Symp. on Combustion, The Combustion Institute, pp. 821-831, 1978.

2. Borghese, A., D'Alessio, A., Russo, G. and Venitozzi, C., "Time-Resolved Electrical and Spectroscopic Study of Very Short Spark Discharges", Int. Symp. on Diagnostics and Modelling of Combustion in Reciprocating Engines, Tokio, pp. 77-83, 1985.

3. Alden, M., Grafström, P., Hertz, H.M., Holmstedt, G.S., Högberg, T., Russberg, G. and Svamberg, S., "Characterization of Ultra-Short High Current Sparks for Ignition Systems", Int. Symp. on Diagnostics and Modelling of Combustion in Reciprocating Engines,Tokio,85-90,1985.

4. Borghese, A., D'Alessio, A., Diana, M., and Venitozzi, C., "Development of Hot Nitrogen Kernel Produced by a Very Fast Spark Discharge", XXII Intern. Symp. on Combustion",Seattle,pp.1651-1659, 1988.

5. Kono, M., Niu, K., Tsukamoto, T. and Ujiie, Y., "Mechanism of Flame Kernel Formation Produced by Short Duration Sparks", XXII Intern. Symp. on Combustion, The Combustion Institute, Seattle, pp. 1643-1649, 1988.

6. Borghese, A., Diana, M., Moccia, V. and Tamai, R., "Early Growth of Flames, Ignited by Fast Sparks", submitted to Combustion Science & Technology, 1990.

7. Borghese, A., Diana, M. and Venitozzi, C., "Optical Diagnostics of Spark-Induced Fluid Dynamics", IX Intern. Conf. on Gas Discharges and Their Applications, Venezia, pp. 569-572, 1988.

8. Borghese, A. and Diana, M., "A Contribution to Spark Ignition Modelling", IX Intern. Conf. on Gas Discharges and Their Applications, Venezia, pp. 579-582, 1988.

9. Landau, L. and Lifchitz, E., "Mecanique des Fluides", Editions MIR, Moscou, p. 493, 1971.

10. Adams, W., Birsztejn, T., Kupe, J.K.Z. and Wilhelmi, H., "Ein neu entwickeltes Plasmastrahlzündsystem zur Verbrennung von Magergemischen", MTZ Motortechnische Zeitschrift 49 (1988) 12, 515-519.